Advances in Astronomy and Space Physics, **2**, 167-172 (2012)

Effects of equatorial chorus wave normal azimuthal distribution on wave propagation

H. Breuillard[1]*, *D. I. Mendzhul*[2], *O. V. Agapitov*[1,2]

[1]LPC2E/CNES and University of Orleans, France
[2]STUDIUM, Loire Valley Institute for Advanced Studies, Orleans-Tours, France
[3]Taras Shevchenko National University of Kyiv, Glushkova ave., 4, 03127, Kyiv, Ukraine

The non-ducted propagation characteristics of the VLF waves in the inner magnetosphere were studied with respect to their frequency, source localization, and initial polar angle between the wave-normal and the background magnetic field and azimuthal angle. The ray tracing software based on multi-components cold plasma approach was developed by use of the Olson-Pfitzer magnetic field model and the GCPM model of plasma density. We described dynamics of the wave-normals direction during its propagation and magnetospheric reflection. We showed that whistler waves can be reflected when lower hybrid resonance frequency becomes greater than the wave frequency: $\omega_{LH} > \omega$. It corresponds to magnetic latitude $\lambda \sim 50^\circ$. The simulation results confirmed the inapplicability of the quasi-longitudinal approximation to describe the propagation of magnetospheric whistlers. The simulation results of chorus emissions propagation, which use realistic distributions of waves on the initial parameters are presented. Particularly, we obtained distributions of chorus emission waves in dependence on the wave-normal directions for different magnetic latitudes, with respect to initial azimuthal angle. It is required for studying diffusive processes in the radiation belts. The results are found to be in a good agreement with the CLUSTER STAFF-SA measurements.

Key words: wave propagation; waves in plasma; wave-particle interactions

INTRODUCTION

The most intense electromagnetic plasma waves observed in the Earth's radiation belts and outer magnetosphere, discrete ELF/VLF chorus emissions, are characterised by rising and falling tones in the few hundred to several thousand Hertz frequency range [11, 29, 30]. See also reviews by [23] and [26] and references therein. Critical to radiation belt dynamics, these emissions have been studied intensively because they play a crucial role in the acceleration of energetic electrons in the outer radiation belt. Typically ELF/VLF chorus emissions are observed near the magnetic equatorial plane in the dawn and dayside outer magnetosphere [23]. They have attracted special attention recently because they were observed as waveforms, allowing determination of their wave normal vector distributions. [11] were the first who determined chorus normal vector distributions using the search coil magnetometer aboard OGO5, near the equator, at geosynchronous altitude. Chorus wave normal directions at $\leq 17^\circ$ magnetic latitudes and L-shells $\sim$7.6 were later studied in [16]. Analysis of the wave normals and the Poynting fluxes for separate emission elements has shown that the emissions are generated in proximity to the geomagnetic equator and propagate to higher latitudes in a non-ducted whistler mode [11, 16] or duct mode [31]. Chorus emissions are usually observed in the Earth's dawn sector between 23:00 and 13:00 MLT [29]. These emissions, which propagate in the whistler mode, consist of two broad frequency bands on either side of half local equatorial gyrofrequency ω_{ce} at the geomagnetic equator along the magnetic field line on which the waves are observed [29, 30]. If present, the upper band exists in the $\omega/\omega_{ce} \approx 0.5{-}0.75$ frequency range and contains discrete chorus elements rising at a few kHz/s. The lower band exists in the $\omega/\omega_{ce} \approx 0.1{-}0.5$ frequency range and contains both elements rising at a few kHz/s and diffuse elements. In the inner magnetosphere, L-shell is $\sim$2–6, wave generation onset has been shown to be associated with substorm electron injections [14]. Chorus in the radiation belts is believed to be generated through electron cyclotron instability when the distribution of energetic electrons in the 5 to 150 keV range is strongly anisotropic [28]. This has been shown to be the case in recent studies of such waves during electron injections. Chorus waves in the outer dayside region have received further attention recently, especially as the THEMIS mission was able to extend previous observations beyond $L \sim 7$ to $L \sim 13$. Dayside quiet-time chorus cannot be explained in the absence of injec-

*hugo.breuillard@cnrs-orleans.fr

tions, however, and remains an area of active study. Other chorus generation occurs in the local minimum magnetic field regions near the dayside magnetopause on the magnetic latitude near $\pm(40°-50°)$ [30]. The spatial and temporal dependencies of high-latitude chorus parameters are considerably different from those of the chorus generated near the magnetic equator. The frequency range of the high-latitude chorus is similar to chorus waves generated near the magnetic equator at $L > 10$ but their spectral power distribution exhibits two maxima: $(0-0.15)\omega_{ce}$ and $(0.25–0.30)\omega_{ce}$. These emissions are mainly detected within 1–2 $R_{\rm E}$ from the magnetopause [30].

Before the CLUSTER mission, observations of ELF/VLF chorus emissions were mainly made by single spacecraft, such as ISEE 1 and ISEE 2, which observed many similar events [15]. Recent Poynting flux and polarization measurements aboard CLUSTER spacecraft confirmed that the chorus source is located close to the equatorial plane [24, 25]. Measurements around the magnetic equator demonstrate the change in sign of the parallel component of the Poynting vector when the satellites cross the equator region. Poynting vector flux analysis indicates that the central position of the chorus source fluctuates along the background magnetic field within 1000–2000 km of the geomagnetic equatorial plane in the timescale of minutes. In studies of chorus emission generation mechanisms, [17] and [28] gave theoretical estimates of the scale size of the wave generation region. Attempts to estimate the scale size experimentally were made using coordinated CLUSTER [3, 4, 25] and more recently THEMIS [1, 2] observations in the radiation belt region.

Although the magnetospheric reflection of whistler chorus is discussed and simulated in a number of papers, such as [17] and [11], experimental confirmation is scarce. Continuous increase in the angle between the wave vector and background magnetic field for several cases of reflected chorus in the outer magnetosphere, based on Ogo 5 measurements, was shown in [11]. In [24] the Poynting vector and wave normal directions of chorus waves were analysed using CLUSTER STAFF-SA measurements of spectral matrices with a 4 s time resolution [3]. Another CLUSTER spacecraft observed waves propagating from the geomagnetic equator region and reflected waves that reached a lower hybrid resonance reflection at low altitudes and returned to the equator at another location with a lower intensity [1]. [24] corroborated this interpretation using ray tracing analysis. [9] demonstrated wave reflection, refraction and resultant inward radial propagation across L-shells and MLT over several R_E. The agreement between models and THEMIS data in the above study [9] encourages use of the ray tracing technique to determine evolution and consequences of chorus waves outside the plasmasphere. To this end it is necessary to develop a numerical ray tracing code that can reproduce wave distributions based on direct measurements and then to fill up the observed distributions by the distributions obtained from simulations.

In this paper we obtain the distribution of chorus wave parameters, taking as a basis CLUSTER observations and to study influence of the equatorial azimuthal wave normal distribution to wave properties at high latitudes.

MODEL DESCRIPTION

In this section, we present the numerical model which computes ray trajectories of chorus emissions (ELF/VLF whistler modes) in the inner magnetosphere using the approximation of the cold collisionless multi-components plasma. The calculation is carried out making use of realistic plasma density parameters and pre-selected initial wave distributions.

The electromagnetic field should be presented in the following form $E, B(\vec{k}, \omega, \vec{r}, t)e^{-i(\omega t - \vec{k}\vec{r})}$, where the field amplitude varies slowly compared to the eikonal φ (written as a four-dimensional line integral). In such approximation $\vec{k} = \nabla\varphi(\vec{r})$ and the equations are transformed into a system of eikonal equations. The Maxwell's equations give a system of equation for $\vec{E}$ components:

$$\widehat{M}\vec{E} = \vec{k}(\vec{k}\vec{E}) - (\vec{k}\vec{k})\vec{E} + \frac{\omega^2}{c^2}\widehat{\varepsilon}. \qquad (1)$$

Then, the condition of solvability gives the dispersion relation:

$$M = \left\| \widehat{M}(\vec{k}, \omega, \vec{r}, t) \right\| = 0.$$

By use of Using the approximation of cold collisionless plasma in the background magnetic field in the field aligned coordinate system where $\vec{B}_0$ is along Z with the angle θ between the wave normal and the background magnetic field $\vec{B}_0$, the dispersion relation has the form [27]:

$$\left(1 - \frac{\omega^2}{\omega_{pe}^2 + \omega_{pi}^2}\right)\left[\left(\frac{\omega}{\omega_{ce}}\left(1 + \frac{\omega_{pe}^2 + \omega_{pi}^2}{c^2k^2 - \omega^2}\right) - \right.\right.$$
$$\left. - \frac{\omega_{ci}}{\omega}\right)^2 - (1-\gamma)^2\Bigg] + \left[1 + \gamma\left(\frac{\omega_{pe}^2 + \omega_{pi}^2}{c^2k^2 - \omega^2} - \right.\right.$$
$$\left.\left. -1 + \gamma\right) - \left(\frac{\omega_{ci}}{\omega}\right)^2\right]\frac{ck\sin\theta}{c^2k^2 - \omega^2} = M = 0, \quad (2)$$

where $\omega_{ce} = \dfrac{eB_0}{cm_e}$ is the local electron gyrofrequency,

$\omega_{pe} = \dfrac{4\pi n e^2}{m_e}$, $\gamma = m_e/m_i = 1/1836.15$. The solutions of the dispersion relation are shown in Fig. 1 for two cases $\omega_{pe} > \omega_{ce}$ and $\omega_{pe} < \omega_{ce}$ respectively. This dispersion relation is used to solve numerically the system of equations for the ray tracing:

$$\frac{d\vec{r}}{dt} = \frac{\partial\omega}{\partial\vec{k}}; \quad \frac{d\vec{k}}{dt} = -\frac{\partial\omega}{\partial\vec{r}}, \tag{3}$$

in the following form:

$$\frac{d\vec{r}}{dt} = -\left(\frac{\partial M}{\partial\vec{k}}\right)\left(\frac{\partial M}{\partial\omega}\right)^{-1}; \qquad \frac{d\vec{k}}{dt} = \left(\frac{\partial M}{\partial\vec{r}}\right)\left(\frac{\partial M}{\partial\omega}\right)^{-1}. \tag{4}$$

The absolute value of the $\vec{k}$-vector can be obtained from the dispersion relation for whistler waves in a form:

$$\left(\frac{kc}{\omega}\right)^2 = \Bigg(RL\sin^2\theta + PS(1+\cos^2\theta) - \Big[\left(RL\sin^2\theta + PS(1+\cos^2\theta)\right)^2 - 4PRL\left(S\sin^2\theta + P\cos^2\theta\right)\Big]^{1/2}\Bigg) \times \left(2\left[S\sin^2\theta + P\cos^2\theta\right]\right)^{-1}, \tag{5}$$

where R, L, P, and S are the polarization parameters, following the notation from [27]:

$$R = 1 - \left(\frac{\omega_{pe}}{\omega_{ce}}\right)^2\left(\frac{\omega_{ce}}{\omega}\right)\left[\left(\frac{\omega_{ce}}{\omega}\right) - 1\right]^{-1},$$

$$L = 1 - \left(\frac{\omega_{pe}}{\omega_{ce}}\right)^2\left(\frac{\omega_{ce}}{\omega}\right)\left[\left(\frac{\omega_{ce}}{\omega}\right) + 1\right]^{-1},$$

$$S = \frac{R+L}{2}, \quad D = \frac{R-L}{2}, \quad P = 1 - \left(\frac{\omega_{pe}}{\omega}\right)^2,$$

where ω_{pe} is the local plasma frequency.

Magnetospheric chorus emissions are commonly observed between $2.5\,R_E$ and $10\,R_E$. Near $2.5\,R_E$ the Earth's core magnetic field is assumed to have a tilted dipolar structure with the dipole magnetic momentum corresponding to year 2005 epoch, and an analytical model includes the contribution of sources external to the Earth (namely magnetopause, tail and ring currents) at larger altitudes [22]. It is valid for all tilts of the Earth's dipole axis during rather quiet magnetosphere ($K_p < 4$), and has been optimized for the near-Earth region (from $2\,R_E$ to $15\,R_E$). To obtain densities of the magnetospheric plasma species throughout the entire volume of the inner magnetosphere we use the Global Core Plasma Model [12] (for more detailed description of the used models see [10]).

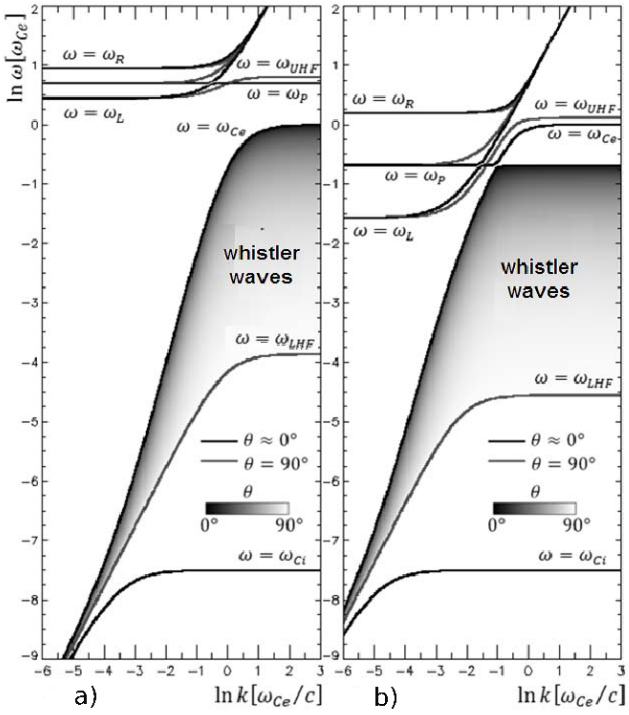

Fig. 1: Dispersion of electromagnetic waves for two cases $\omega_{pe} > \omega_{ce}$ (a) and $\omega_{pe} < \omega_{ce}$ (b).

CHORUS WAVE NORMAL PROPERTIES IN THE OUTER RADIATION BELT

The behaviour of the numerical distribution of poleward rays is thus very consistent with the observed distribution presented in Fig. 2e from [4, 5], where the same wave normal angle distribution is constructed using the CLUSTER STAFF-SA measurements from years 2001 to 2010. The good agreement is confirmed [10]. The distributions obtained from experimental data and as a result of numerical simulations both exhibit the same tendency, i. e. a rapid increase of the mean value and variance with the growth of λ. It was shown that starting with $\vec{k}$ direction close to the direction of the background magnetic field near the equator, wave-normals diverge from field aligned direction very fast and already on $\lambda \approx 25^\circ - 35^\circ$ became close to the resonance cone (Fig. 2, 3). When the wave frequency becomes less than the background lower hybrid frequency, $\omega_{LH} \simeq \left(\frac{1}{\omega_{ce}\ omega_{ci}} + \frac{1}{\omega_{pi}}\right)^{-1}$, whistler wave transforms to the quasi-electrostatic mode, wave-normal comes to transverse direction, group velocity

changes its sign and wave can be reflected [2]. From the numerical simulation of chorus emission propagation we obtained distributions of chorus emission waves in dependence on the wave-normal directions for different magnetic latitudes. The deviation of the wave-normal direction from the direction of the background magnetic field tends to significant increase of the efficiency of the wave-particle interaction in the radiation belts [6, 7]. Due to particle scattering on chorus waves the electron life-time decreases [20, 21]. The wave normal distributions obtained using the hot plasma approximations are described in [10].

Fig. 3 shows the wave power distribution of θ^* as a function of λ, where $\theta^* = \theta \cos\phi$, for chorus waves generated at the equator. Here ϕ is defined as the wave-vector azimuthal angle. Thus, the rays that are initially oriented towards the Earth (i. e. $90° < \phi_0 < 180°$, in blue lines) have a negative initial θ^* at the equator, whereas rays initially directed outward (i. e., $0° < \phi_0 < 90°$, in red lines) have a positive θ_0^*. From this figure it can be seen that rays quickly defer outward during their propagation, as none is directed towards the Earth above $\lambda = 40°$. Therefore, the majority of rays generated inward intersect the direction of the local magnetic field for $\lambda < 15°$, which explains the observed strong population of quasi-parallel waves at these low latitudes. For large initial angles, these rays ($-30° < \theta_0^* < -15°$) can also propagate quasi-parallel to the magnetic field up to latitudes $\sim 30°$, whereas rays initially launched outward quickly tend to resonance cone ($\lambda > 20°$). However, the two ray populations quickly merge and this overlapping forms the major part of the distribution, especially at high latitudes, that propagates obliquely, which is consistent with CLUSTER observations [5].

The field aligned population of waves is seen in the spacecraft data at $\lambda \simeq 20° - 30°$. The ray tracing does not show such a group of waves. This can be seen also from the angle ψ between the spacecraft position vector $\vec{r}$ and wave normal shown in Fig. 4. ψ is distributed near 90° at the equator, and from ray tracing decreases with λ to $\sim 60° - 70°$ (Fig. 4b). Ray tracing well reproduces ψ distribution from the spacecraft observations shown in Fig 4a. Chorus wave normals tend to rotate outward from the Earth due to magnetic field lines curvature and magnetic field absolute value gradient. The field aligned direction is indicated with black dashed line and the field aligned wave population is observed in ψ distribution at $\lambda \approx 10° - 30°$. This population of field aligned waves cannot be obtained from the geometric optics approximation used in our paper, though a very small population of quasi-parallel waves is produced by ray tracing simulations at these latitudes. The Landau damping is more effective for the oblique waves and wave amplification is more effective for field aligned waves. The wave amplification and wave damping during the propagation can result in the observed differences between spacecraft observations and numerical simulations and they have to be taken into account, that will be the subject of the future work.

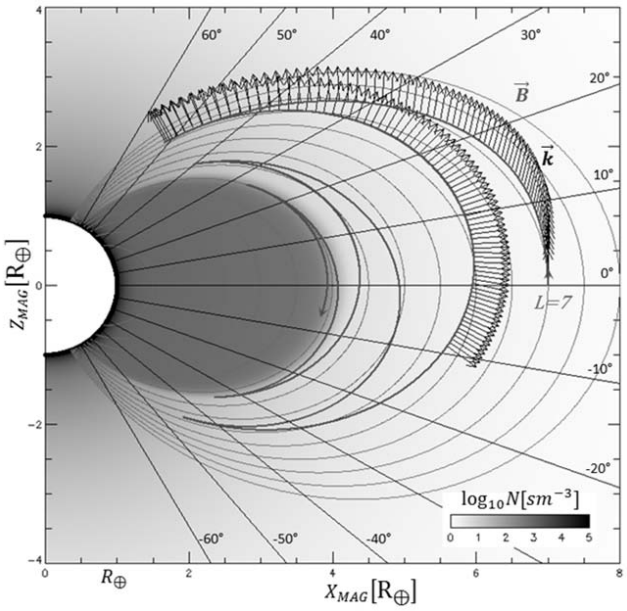

Fig. 2: Ray trace of the whistler wave, generated in the vicinity of the geomagnetic equator with wave-normal directed along the background magnetic field. The wave-normal direction along the trajectory is shown by arrows. The model plasma density (the diffusion equilibrium model) and magnetic field line are shown in grey shades.

CONCLUSIONS

In this paper we present a ray tracing technique for the cold magnetized multi-components collisionless plasma that has been developed including realistic plasma density and magnetic field models. Ray tracing was carried out assuming that the wave source is situated at equator. The initial distribution of waves in frequencies and in $\vec{k}$-vectors in the source region was chosen to correspond to statistical distribution dependencies on $\vec{k}$-vectors and frequencies obtained from observations. To this end the weight functions corresponding to distributions inferred from observations were applied to initial set of rays [10].

Then, making use of our numerical database we show that it is possible to reconstruct chorus wave-normal distributions as a function of magnetic latitude using weight functions on equator (obtained from experiment). The results of our calculations are in a good agreement with statistical distributions found using ten years observational data measured onboard CLUSTER spacecrafts in [4, 5].

Chorus wave normal angle distribution at the equator peaks at $\theta \approx 15^\circ - 17^\circ$ and θ tends to increase fast with latitude reaching the resonance cone at $\lambda \approx 30^\circ - 40^\circ$ and can be reflected at $\lambda \approx 40^\circ - 45^\circ$ where the wave frequency becomes less than the local lower hybrid frequency. Chorus wave normals tend to rotate outward from the direction to the Earth due to the background magnetic field lines curvature and gradients of magnetic field and plasma density. Thus, waves that are generated towards the Earth can propagate quasi-parallel to the magnetic field up to relatively large latitudes $\lambda \approx 10^\circ - 25^\circ$. These waves could be more easily amplified by resonant interaction with the radiation belts energetic electrons [18, 19] to form the observed field aligned population at these latitudes.

In addition, Landau damping, which is much more effective for oblique wave normal angles [13], tends to decrease the amplitude of oblique chorus waves during their propagation and also results in the concentration of the wave normal distribution near field aligned direction at $\lambda \approx 20^\circ - 35^\circ$. The discrepancies of distributions obtained from the spacecraft observations and from ray tracing can thus be explained presumably by a combination of quasi-parallel wave amplification and Landau damping of oblique waves during chorus waves propagation [8]. Therefore, the existence of an anisotropy in the equatorial azimuthal angle distribution can lead to drastic changes in the wave normal angle distribution. Nevertheless, the statistical majority of oblique wave population in the outer radiation belts, especially at high latitudes, tends to more effective electron scattering [6] and decreasing of electron life-time, especially in the L- shell range from 3 to 5.5 [20].

REFERENCES

[1] Agapitov O., Krasnoselskikh V., Zaliznyak Yu. et al. 2010, Ann. Geophys., 28, 1377

[2] Agapitov O., Krasnoselskikh V., Zaliznyak Yu. et al. 2011, Ann. Geophys., 29, 541

[3] Agapitov O., Krasnoselskikh V., Dudok de Wit T. et al. 2011, J. Geophys. Res., 116, A09222

[4] Agapitov O., Krasnoselskikh V., Khotyaintsev Y. V. & Rolland G. 2011, Geophys. Res. Lett., 38, L20103

[5] Agapitov O., Krasnoselskikh V., Artemyev A. et al. submitted to J. Geophys. Res.

[6] Artemyev A., Agapitov O., Breuillard H., Krasnoselskikh V. & Rolland G. 2012, Geophys. Res. Lett., 39, L08105

[7] Artemyev A., Agapitov O., Krasnoselskikh V., Breuillard H. & Rolland G. 2012, J. Geophys. Res., 117, A08219

[8] Bortnik J., Inan U. S. & Bell T. F. 2006, Geophys. Res. Lett., 33, L03102

[9] Bortnik J., Li W., Thorne R. M. et al. 2009, Science, 324, 775

[10] Breuillard H., Zaliznyak Y., Krasnoselskikh V. V. et al., Ann. Geophys., in press

[11] Burton R. K. & Holzer R. E. 1974, J. Geophys. Res., 79, 1014

[12] Gallagher D. L., Craven P. D. & Comfort R. H. 2000, J. Geophys. Res., 105, 18819

[13] Ginzburg, V. L. and Rukhadze, A. A. 'Waves in magnetoactive plasma', 1975.

[14] Goldstein B. E. & Tsurutani B. T. 1984, J. Geophys. Res., 89, 2789

[15] Gurnett D. A., Anderson R. R., Scarf F. L., Fredricks R. W. & Smith E. J. 1979, Space Sci. Rev., 23, 103

[16] Hayakawa M., Hattori K., Shimakura S., Parrot M. & Lefeuvre F. 1990, Planet. Space Sci., 38, 135

[17] Helliwell R. A. 'Whistlers and related ionospheric phenomena', 1965, Stanford University Press, USA

[18] Kennel C. F. & Thorne R. M. 1967, J. Geophys. Res., 72, 871

[19] Kennel C. F. & Petschek H. E. 1966, J. Geophys. Res., 71, 1

[20] Mourenas D., Artemyev A. V., Ripoll J.-F., Agapitov O. V. & Krasnoselskikh V. V. 2012, J. Geophys. Res., 117, A06234

[21] Mourenas D., Artemyev A., Agapitov O. & Krasnoselskikh V. 2012, J. Geophys. Res., 117, A10212

[22] Olson W. P. & Pfitzer K. A. 1974, J. Geophys. Res., 79, 3739

[23] Omura Y., Matsumoto H., & Nunn D. & Rycroft M. J. 1991, J. Atmos. Terr. Phys., 53, 351

[24] Parrot M., Santolík O., Gurnett D., Pickett J. & Cornilleau-Wehrlin N. 2004, Ann. Geophys., 22, 2597

[25] Santolík O., Gurnett D. A., Pickett J. S., Parrot M. & Cornilleau-Wehrlin N. 2005, Planet. Space Sci., 53, 299

[26] Sazhin S. S. & Hayakawa M. 1992, Planet. Space Sci., 4, 681

[27] Stix T. H. 'The Theory of Plasma Waves', 1962, New York, McGraw-Hill

[28] Trakhtengerts V. Y. 1999, Ann. Geophys., 17, 95

[29] Tsurutani B. T. & Smith E. J. 1974, J. Geophys. Res., 79, 118

[30] Tsurutani B. T. & Smith E. J. 1977, J. Geophys. Res., 82, 5112

[31] Yearby K. H., Balikhin M. A., Khotyaintsev Yu. V. et al. 2011, Ann. Geophys., 29, 1629

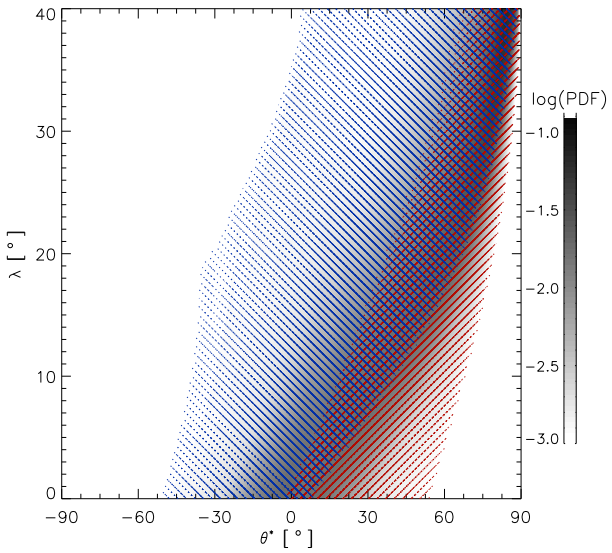

Fig. 3: Density probability function of $\theta^* = \theta \cos\varphi$ as a function of latitude λ for direct chorus waves generated at the equator. The two different ray populations included in the PDF, i. e. rays for which $90° < \varphi_0 < 180°$ and $0° < \varphi_0 < 90°$, are indicated by left and right rotated lines used to fill contours, respectively. The distribution intensity of each population is represented by the thickness of the lines. The colour figure is available in the electronic version of the paper.

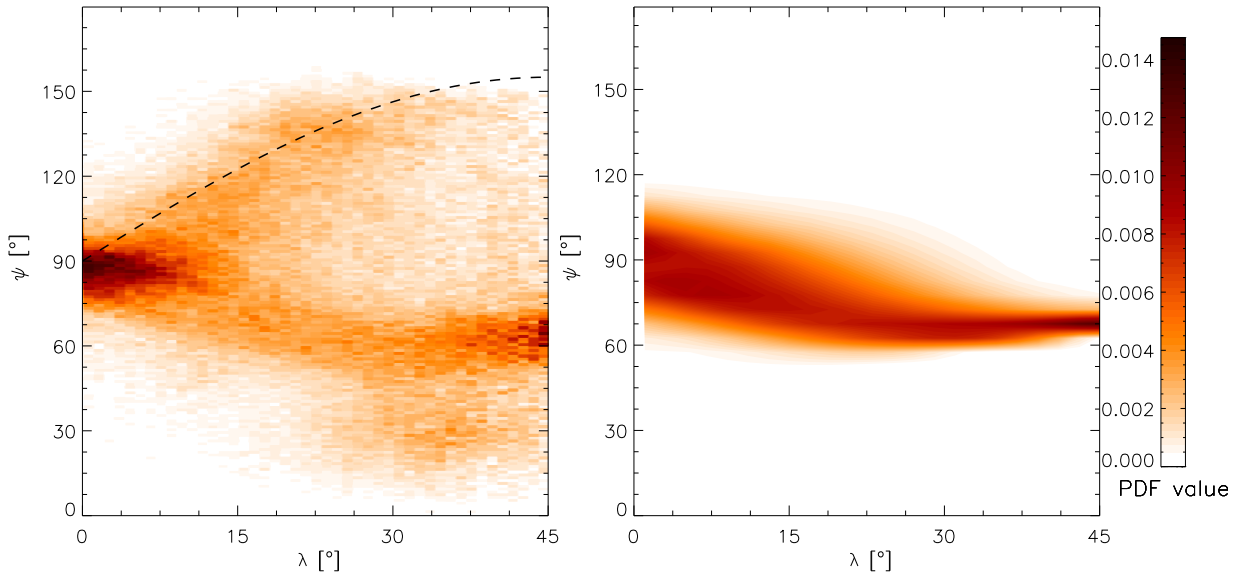

Fig. 4: The PDF of ψ distribution (X axis) as a function of magnetic latitude λ (Y axis) for all computed rays, using Eq.(4) as initial weight function. Distributions are obtained from CLUSTER experimental data (left panel) and numerical simulations (right panel). The colour figure is available in the electronic version of the paper.